



# Biochanin A, as the Lrg1/TGF- $\beta$ /Smad2 pathway blockade, attenuates blood-brain barrier damage after cerebral ischemia-reperfusion by modulating leukocyte migration patterns

LONGSHENG FU<sup>1</sup>; JINFANG HU<sup>1</sup>; FENG SHAO<sup>2</sup>; YAOQI WU<sup>1</sup>; WEI BAI<sup>3</sup>; MINGJIN JIANG<sup>3</sup>; HAO CHEN<sup>4</sup>; LIHUA CHEN<sup>2</sup>; YANNI LV<sup>1,\*</sup>

<sup>1</sup> Department of Pharmacy, The First Affiliated Hospital of Nanchang University, Nanchang, 330006, China

<sup>2</sup> Key Laboratory of Modern Preparation of TCM, Ministry of Education, Jiangxi University of Traditional Chinese Medicine, Nanchang, 330006, China

<sup>3</sup> Translational Medicine Institute of Jiangxi, The First Affiliated Hospital of Nanchang University, Nanchang, 330006, China

<sup>4</sup> Neurology Department, The First Affiliated Hospital of Nanchang University, Nanchang, 330006, China

**Key words:** Biochanin A, Blockade, Leukocyte migration, Blood-brain barrier damage, Ischemia-reperfusion, Lrg1

**Abstract: Background:** Biochanin A is an excellent dietary isoflavone that has the concomitant function of both medicine and foodstuff. The attenuation function of biochanin A on blood-brain barrier (BBB) damage induced by cerebral ischemia-reperfusion remains unclear. **Methods:** C57BL/6 mice were subjected to 1 h middle cerebral artery occlusion (MCAO) followed by 24 h reperfusion. The infarct volume of the brain was stained by TTC, while leakage of the brain was quantitatively stained by Evans blue, and the neurologic deficit score was measured. Microglial-induced morphologic changes were observed via immunofluorescence staining, and rolling and adhering leukocytes in venules were observed via two-photon imaging, while the inner fluorescein isothiocyanate-albumin of venules were compared with those of surrounding interstitial area through venular albumin leakage. **Results:** The attenuation effect of biochanin A on tight junction injury was compared in ischemia-reperfusion mice or conventional knockdown of leucine-rich  $\alpha$ 2-glycoprotein 1 (Lrg1) mice. Biochanin A could ameliorate BBB injury in mice with cerebral ischemia-reperfusion in a dose-dependent manner by strengthening the immunostaining volume of occludin, claudin-5, and zonula occludens-1. The amoeba morphologic changes of microglial combined with the elevated expression of Lrg1 could be relieved under the treatment of biochanin A. Biochanin A played a countervailing role on the rolling leukocytes in the vessel, while the leakage of blood vessels was reduced. Biochanin A diminished its functions to further improved attenuation for tight junction injury on conventional Lrg1-knockout mice, as well as the inhibition effects on TGF- $\beta$ 1, and the phosphorylation of suppressor of mothers against decapentaplegic 2 (Smad2)/Smad2 via western blot assay. **Conclusion:** Biochanin A could alleviate tight junction injury induced by cerebral ischemia-reperfusion and blocked the Lrg1/TGF- $\beta$ /Smad2 pathway to modulate leukocyte migration patterns.

## Introduction

Cerebral ischemia is a serious disease threatening human health. According to the 2021 international conference on cerebrovascular diseases at the Tiantan International Stroke Conference, China has nearly 2 million new cases every year. Approximately 85% of cerebrovascular diseases were ischemic stroke, with the characteristics of high morbidity and mortality and a high disability rate. It is difficult to improve cerebral circulation through existing clinical treatment methods, such as thrombolysis and antiplatelets,

even when blood reperfusion occurs, and may even cause further damage to the structure and function of the blood-brain barrier (BBB) (Mendelson and Prabhakaran, 2021). BBB protects from the inflammatory signaling molecules under physiological status and plays an important role in repairing brain injury. After BBB is damaged, a series of energy metabolism disorders and inflammatory cascade reactions occur, causing further damage to the BBB structure and function, aggravating ischemia, brain neurological impairment and sequelae (Lv and Fu, 2018). The damage to BBB is further aggravated by the microglia-induced entrance of rolling leukocytes into vessels that possibly contribute to the inflammatory injury (Otxoa-de-Amezaga et al., 2019). Therefore, maintaining the tightly connected structure and inhibiting the potential

\*Address correspondence to: Yanni Lv, yannilv225@ncu.edu.cn

Received: 18 December 2022; Accepted: 14 April 2023;

Published: 28 August 2023



inflammatory injury of vascular endothelial cells in ischemia-reperfusion areas is of great significance to the occurrence and development of ischemia-reperfusion injury.

Stroke ranks first among the causes of death of Chinese residents. However, the treatment of stroke is still a difficult problem in the current medical field. The number of stroke patients in China exceeds 25 million, and the cost of stroke-related drugs exceeds 20 billion yuan/per year, with a huge potential market. Currently, more than 400 stroke-related drugs are available, although the number of really effective and safe drugs is very limited. Thus, there is still a need to develop effective and safe medicines, especially from ingredients in traditional Chinese medicine. The advantages of natural products, especially traditional Chinese medicines, include their high efficiency and low toxicity. A versatile compound—biochanin A, demonstrates multiple effects in angiogenesis, cellular growth, and cell apoptosis (Sarfraz *et al.*, 2020). The attenuation function of biochanin A on tight junction injury induced by ischemia-reperfusion is little known. Leucine-rich  $\alpha$ 2-glycoprotein 1 (Lrg1) is a member of the leucine-rich repeat family. Lrg1 has a major role in many diseases, such as respiratory, hematological, blood diseases, etc. (Zou *et al.*, 2022). It was confirmed to regulate the upstream of the transforming growth factor- $\beta$  (TGF- $\beta$ ) signaling pathway (Zou *et al.*, 2022). In recent years, while studies on the action of Lrg1 in neurological diseases have advanced rapidly, very few have paid attention to the association between Lrg1 and tight junction injury. This study aimed to elucidate the underlying role of biochanin A in triggering the Lrg1 signaling pathway in tight junction injury in cerebral ischemia-reperfusion.

## Materials and Methods

### Materials and chemicals

Biochanin A and nimodipine, with a peak area normalization rate of 98.8% via HPLC, were purchased from Nanjing Zelang Pharmaceutical Co., Ltd., China

### Animals

C57BL/6 mice weighing 18–22 g were obtained from the Yangzhou University Model Animal Research Center (certificate No. SCXK 2018-0004). Mice were reared at Nanchang University Laboratory with 12 h light-dark cycle conditions and optimal temperature and humidity. Lrg1<sup>-/-</sup> mice with a C57BL/6 background were originally generated at Cyagen Biosciences Corporation by mating the knockout (KO) mouse (Strain number: C57BL/6N-Lrg1<sup>em1cyagen</sup> and Strain name: KOCMP-76905-Lrg1-B6N-VA). The Lrg1 gene (NCBI Reference Sequence: NM\_029796; Ensembl: ENSMUSG00000037095). Exon 1 and the TGA stop codon in exon 2 (Transcript: NSMUST00000041357) were selected as target sites. Cas9 and gRNA were co-injected into fertilized eggs for KO mouse production. The pups were genotyped by polymerase chain reaction followed by sequencing analysis. Exon 1 starts from 2 bp of KO region. Exon 1~2 covers 100.0% of the coding region. The size of the effective KO region was ~1940 bp. The KO region does not have any other known gene. Lrg1<sup>-/-</sup> mice were

backcrossed to C75BL/6N mice for four generations (3 months, 18–22 g) and raised in a specific pathogen-free laboratory of Nanchang University (SYXK (Gan) 2021-0003). All procedures were performed in accordance with the National Institutes of Health Guidelines for the Use of Laboratory Animals, accompanied by minimizing the pain the animals suffered. Laboratory animal ethics were approved by Institutional Animal Care and use Committee of The First Affiliated Hospital of Nanchang University at December 02, 2022 (No. 202212214).

### Cerebral ischemia-reperfusion and animal group

C57BL/6 mice were anesthetized with 1.2% isoflurane, while the body temperature was maintained at 37°C during the ischemia period. A blunt 6–0 nylon monofilament was inserted into the proximal external carotid stump and advanced 8–10 mm towards the internal carotid artery to block the middle cerebral artery. After 1 h of occlusion, the nylon monofilament was withdrawn from the carotid artery, while 24 h reperfusion was followed immediately afterwards. The sham-operated mice underwent the same procedure, but the suture did not advance into the internal carotid artery. A laser Doppler flowmeter (LDF, FLPI2, Moor, London, England) was applied to confirm that the middle arterial blood flow of the brain dropped to less than 30% of the basic cerebral blood flow immediately after occlusion. Animals whose blood flow dropped below 30% of pre-ischemia levels were used for further experiments.

In protocol 1, mice were randomly categorized into five groups (10–12 wild-type mice were randomly assigned to each group, and finally 8 wild type mice with successful modeling were entered into the result analysis for each group): (1) sham-operated mice, (2) mice exposed to 1 h of ischemia, 24 h of reperfusion stroke, (3) mice exposed to 1 h of ischemia, 24 h of reperfusion stroke and treated with a low dose of biochanin A (5 mg/kg), (4) mice exposed to 1 h of ischemia, 24 h of reperfusion stroke, and treated with a middle dose of biochanin A (10 mg/kg), (5) mice exposed to 1 h of ischemia, 24 h of reperfusion stroke, and treated with a high dose of biochanin A (20 mg/kg). The sham-operated group underwent the same procedure but without interposition to sever the left middle cerebral artery. The biochanin A treatment group was administered intragastrically with 5, 10, 20 mg/kg biochanin A, and 10 mg/kg nimodipine (Lv and Fu, 2018) (dissolved in NaCl) at the onset of 1 h of cerebral ischemia and then received additional injections every 24 h during the experimental period, whereas the sham-operated group was administered intragastrically with a solution of equivalent volume NaCl.

For protocol 2, mice were randomly divided into six groups (10–12 wild-type or conventional knockout mice were randomly assigned to each group, finally, 8 successful mice model in each group were selected for the analysis of the results): (1) sham-operated WT (wild type) mice, (2) sham-operated KO (conventional knockout of Lrg1) mice, (3) middle cerebral artery occlusion (MCAO) WT mice exposed to 1 h of ischemia and 24 h of reperfusion stroke, (4) MCAO KO mice exposed to 1 h of ischemia and 24 h of reperfusion stroke, (5) MCAO WT mice exposed to 1 h of ischemia, 24 h of reperfusion, and treated with biochanin A

(20 mg/kg); (6) MCAO KO mice exposed to 1 h of ischemia, 24 h of reperfusion stroke KO mice and treated with biochanin A (20 mg/kg). The sham-operated group underwent the same procedure but without interposition to sever the left middle cerebral artery. The biochanin A treatment group was intragastrically administered with 5, 10, or 20 biochanin A (dissolved in NaCl) at the onset of 1 h of cerebral ischemia and then received additional injections every 24 h during the experimental period, whereas the sham-operated group was administered intragastrically with a solution of equivalent volume NaCl. At the end of the ischemia-reperfusion period, the brain tissues in the ischemia region collected from each group were subjected to Evans blue (EB) leakage, infraction volume calculation, immunofluorescence staining, rolling and adhering leukocytes in venules, cerebral blood flow, venular albumin leakage, and western blot assay.

#### *Evaluation of blood-brain barrier permeability*

EB (Sigma-Aldrich Co., Saint Louis, USA) was dissolved in 0.9% NaCl solution at 2% per 10 g body weight and injected into the tail vein of each mouse 2 h before the animals were euthanized. For the quantitative measurement of EB leakage, the ipsilateral hemispheres were removed, homogenized in 1 mL of trichloroacetic acid, and centrifuged at 12,000 rpm for 20 min. The EB concentration was quantitatively determined by measuring the absorbance of the supernatant at 620 nm using a spectrophotometer. A standard curve was used to quantify the EB content as EB  $\mu\text{g/g}$  tissue. During cerebral ischemia-reperfusion, anesthesia was administered with 1.2% isoflurane and then 0.9% NaCl solution was injected through cardiac perfusion. To quantitatively measure EB leakage, the ischemia hemisphere was removed, homogenized in 1 mL trichloroacetic acid, and centrifuged at 12,000 rpm for 20 min. EB leakage was quantitatively measured as mentioned in this section.

#### *Measurement of the infarct volumes*

At the end of operation, the brains were quickly dissected into 2 mm/per section from the coronal position. Brain slices were incubated in 2% 2,3,5-triphenyltetrazole sodium chloride (TTC) solution in phosphate buffered-saline (PBS) at 37°C for 20 min. Normal brain areas stained with TTC appeared red, but infarct areas appeared white. Stained sections were observed under Canon sx20 high-resolution digital camera (Canon, Tokyo, Japan). The infarct volume was computerized through Motic Med 6.0 image analysis.

#### *Neurologic deficit score*

The neurologic deficit score was evaluated on an 18-point scale. Mice were tested after 24 h of reperfusion based on the Longa score system: 0, asymptomatic; 1, mice could not extend the opposite fore limb when lifting the tail; 2, mice could not rotate to the damaged side; 3, mice tipped uncontrollably to the opposite side; 4, mice could not perform a normal walk or loss of consciousness. Each evaluation score was added to the final total score of neurologic deficits.

#### *Hematoxylin and eosin (H&E) staining*

Mice were anesthetized following 1 h of ischemia and 24 h of reperfusion and perfused transcardially with 0.9% NaCl and 4% paraformaldehyde through the left ventricle. After the brain was removed, it was post-fixed in cold 4% paraformaldehyde at 4°C for 24 h. Following dehydration, the specimens were embedded in paraffin, cut into 5-mm sections, and stained with H&E. The histological morphology of each brain specimen was examined by optical microscopy.

#### *Immunofluorescence staining of brain tissues*

Each group of brain tissues in the ischemic region was sliced into 5 mm thick slices. After being washed with phosphoric acid buffered brine (pH 7.4), the slices were incubated with cold ethanol at 4°C for 10 min and immobilized with 10% normal goat serum, 3% bovine serum albumin, and 0.1% Triton X-100 in PBS for 1 h. Then, they were incubated with the Lrg1 (DF4136, Biosciences, Shanghai, China), ionized calcium-binding adapter molecule 1 (IBA1; ab178847, Abcam, Cambridge, UK), occludin (ab216327, Abcam, Cambridge, UK), claudin-5 (ab131259, Abcam, Cambridge, UK), and zonula occludens-1 (ZO-1; ab96587, Abcam, Cambridge, UK) primary antibody (immunofluorescent for 1: 100) for 48 h at 4°C. After washing, brain tissues were separately incubated overnight with Alexa Fluor® 488 conjugated donkey anti-goat IgG (H +L) antibody (ab150129, Abcam, Cambridge, UK, 1:2000) at 4°C. The wash step was repeated, and the nuclei of all cells were washed and incubated with 4',6-diamidino-2-phenylindole (DAPI, ab104139, Abcam, Cambridge, UK, 1:1000) for 15 min.

#### *Histological assessment of occludin, claudin-5, and zonula occludens-1*

The ischemia brain tissues were fixed with 4% paraformaldehyde for 24 h and then embedded with paraffin after dehydration. A series of 5 mm thick slices were incubated with anti-occludin, claudin-5, and ZO-1 antibodies (rabbit polyclonal IgG, 1:50, Abcam, Cambridge, UK). A 3-CCD color camera was used to digitize each section containing eight ischemia boundary areas under a 20 × objective lens. Quantitatively, cells or regions positive for occludin, claudin-5, and ZO-1 were measured in 20 enlarged vessels. The expression of occludin, claudin-5, and ZO-1 in the ischemia boundary region was digitally measured using Olympus BX40. The data are shown as the number of positive cells or the percentage of the vascular area or ischemia border area.

#### *Rolling and adhering leukocytes in venules*

Fluorescent tracer Rhodamine 6G was administered (5 mg/kg) via the femoral vein 10 min before the MCAO operation. The cerebral cortex venules in the ischemic region were observed under an intravital microscope (BX51WI, Olympus, Tokyo, Japan), while lighting with a mercury lamp and analyzing in slow-motion videos. The leukocytes attached to the venular wall for more than 30 s were identified as adhering

leukocytes. The flickering fluorescence staining cells were identified as the rolling leukocyte streaming in the venules (Wang *et al.*, 2015). The number of adhering and rolling leukocytes was counted in a limited 200  $\mu\text{m}$ /venule. Selected venules were observed under  $\times 400$  magnified view.

#### Venular albumin leakage

Fluorescein isothiocyanate (FITC)-albumin was infused (50 mg/kg) via the femoral vein 10 min before the MCAO operation. The fluorescence of albumin leakage in the ischemic region was observed under an upright microscope for intravital experiments (BX51WI, Olympus, Tokyo, Japan). FITC-albumin fluorescence intensity was measured in selected venules cava (Iv) and surrounding interstitial area (Ii). The proportion of Ii/Iv was compared with the baseline of venules under sham operation condition (Chen *et al.*, 2016). Selected venules were observed under  $\times 400$  magnified view.

#### Cerebral blood flow

Cerebral blood flow was measured under a LDF (FLPI2, Moor, London, UK). After exposure of the skull, a decrease in the blood flow was observed in the ischemia-reperfusion area. The area of the ischemia-reperfusion with blood flow was selected. Each pixel on the blood flow map was red for high

measurement and blue for low measurement. The average value of blood flow in the area was calculated, and the unit of blood flow is the perfusion unit (PU).

#### Western blot analysis

Protein samples (40 mg) collected from brain tissues in the ischemic region were separated via 12.5% sodium dodecyl sulfate polyacrylamide gel electrophoresis assay. The proteins were subsequently transferred to polyvinylidene fluoride membranes in a tris-glycine transfer buffer. The membranes were blocked with 5% nonfat dry milk for 2 h at room temperature and then probed with anti-Lrg1 (DF4136, Biosciences, Shanghai, China), anti-TGF- $\beta$ 1 (ab215715, Abcam, Cambridge, UK), anti-p-suppressor of mothers against decapentaplegic 2 (Smad2; ab280888, Abcam, UK), anti-Smad2 (ab40855, Abcam, Cambridge, UK), anti-occludin, anti-claudin-5, anti-ZO-1, and  $\beta$ -actin primary antibodies (WB for 1: 1000) at 4°C overnight, and then incubated with appropriate horseradish peroxidase-conjugated secondary antibody (ab6728, Abcam, Cambridge, UK, 1:2000) for 50 min. Enhanced chemiluminescence was utilized to display the bands, and the images of the bands were captured based on a biological image analysis system (Bio-Rad, Hercules, California, USA).

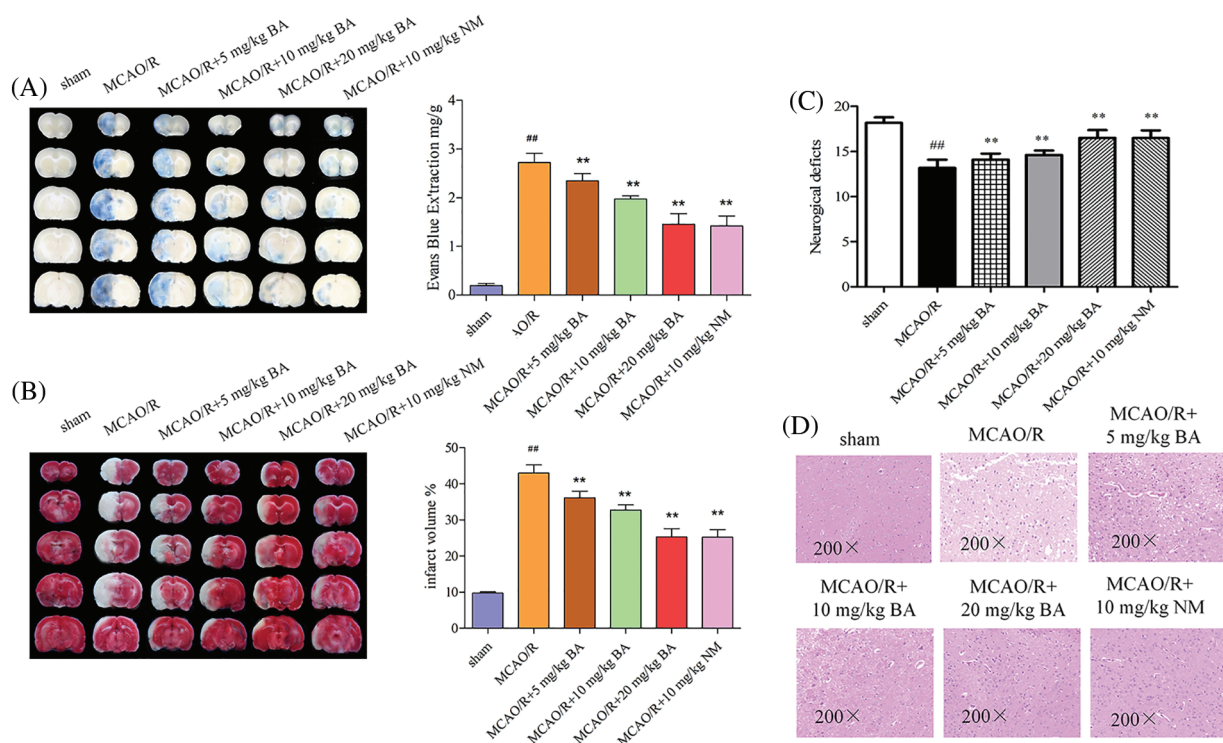


**FIGURE 1.** Effects of biochanin A on blood-brain barrier permeability and infarct volume induced by ischemia-reperfusion injury. Nimodipine (10 mg/kg) was administrated as the positive control (Lv and Fu, 2018). (A) Representative gross appearance and quantitative analysis of Evans blue-stained brains exposed to 1 h of ischemia and 24 h of reperfusion. (B) Representative cerebral tissues and quantitative analysis of 2,3,5-triphenyltetrazole sodium chloride-stained brains subjected to ischemia-reperfusion. (C) The neurologic deficit score for each group was evaluated. (D) Representative cerebral tissues were processed for hematoxylin and eosin staining under a magnification of  $\times 200$ . Results included eight independent experiments, and the data represent the mean  $\pm$  SD,  $n = 8$ . <sup>##</sup> $p < 0.01$  vs. sham mice, <sup>\*\*</sup> $p < 0.01$  vs. ischemia-reperfusion mice. Sham, sham-operated mice; MCAO, mice exposed to 1 h of ischemia and 24 h of reperfusion; BA, mice treated with biochanin A; NM, mice treated with nimodipine.

### Statistical analysis

All values are expressed as mean  $\pm$  SD and analyzed by a two-tailed student's *t*-test (two groups) or a two-way ANOVA followed by Bonferroni's test (three or more groups). The significance level was set at  $p < 0.05$  and  $p < 0.01$ .

## Results

### *Biochanin A alleviated the leakage of the blood-brain barrier and reduced infarct volume induced by ischemia-reperfusion injury*

Quantitative staining assay showed EB leakage in the ischemia-reperfusion side of the brain ( $2.73 \pm 0.19$  mg/g,  $p < 0.01$ ) compared with that of the sham-operated group ( $0.19 \pm 0.05$ ). Biochanin A gradually reduced EB leakage (5 mg/kg, 10 mg/kg, and 20 mg/kg biochanin A:  $2.35 \pm 0.14$  mg/g,  $p < 0.01$ ,  $1.98 \pm 0.06$  mg/g,  $p < 0.01$ ,  $1.46 \pm 0.21$  mg/g,  $p < 0.01$ ; nimodipine:  $1.42 \pm 0.20$  mg/g,  $p < 0.01$ ) in a dose-dependent manner (Fig. 1A). For the volume detected following 1 h of ischemia and 24 h of reperfusion, the unstained sections represented the infarct volume. Ischemia-reperfusion mice administered with biochanin A exhibited a much smaller infarct volume (5 mg/kg, 10 mg/kg, and 20 mg/kg biochanin A:  $36.16 \pm 1.81\%$ ,  $p < 0.01$ ,  $32.74 \pm 1.43\%$ ,  $p < 0.01$ ,  $25.32 \pm 2.27\%$ ,  $p < 0.01$ ; nimodipine:  $25.24 \pm 2.06$  mg/g,  $p < 0.01$ ) compared with that of the ischemia-reperfusion mice ( $9.76 \pm 0.33\%$ , Fig. 1B). Neurologic scores decreased after cerebral ischemia-reperfusion, accompanied with paralysis and mobility impairment of the part of the limb, while the limb dysfunction could be partially improved by biochanin A or nimodipine (Fig. 1C). Neuronal cells in the ischemia-reperfusion brain tissues appeared shrunken and showed condensed nuclei and cavitation structure, and this phenotype was ameliorated by biochanin A or nimodipine treatment (Fig. 1D).

### *Biochanin A inhibited Lrg1 activation and leukocyte migration induced by ischemia-reperfusion*

Microglia activation via ischemia-reperfusion facilitated the entrance of leukocytes into the blood and their rolling and adhering to vessels. The response following ischemia-reperfusion could transform the normal microglia to an amoeba-like shape. IBA1 for microglia was visualized with the expression of green fluorescence, and a consistent increasing expression trend was observed for Lrg1 (Fig. 2A, red). Video images of vessels were played back to detect the adhering and rolling leukocytes in a vessel. Rhodamine 6G was applied to rolling and rapidly flowing leukocytes through the vessel; the adhering leukocytes that remained stationary along the vessel for at least 30 s were also quantified (Fig. 2B). Leukocytes were detected by a significant elevation in the rolling velocity in the brain vessels of ischemia-reperfusion mice  $38.90 \pm 12.73$  cell/mm<sup>2</sup> compared to that of the sham mice  $11.33 \pm 8.55$  cell/mm<sup>2</sup> (Fig. 2B). The histogram also showed a significant reduction in adhering rolling leukocytes in ischemia-reperfusion mice ( $5.17 \pm 2.52$  cell/mm<sup>2</sup>,  $p < 0.01$ ) compared with sham mice, at 0 cell/mm<sup>2</sup> (Fig. 2B). Therefore, ischemia-reperfusion stroke could induce the increase in acquisition of leukocytes in the vessels, which

accelerated the rolling rate of the rolling leukocytes. Different doses of biochanin A (5 mg/kg, 10 mg/kg, 20 mg/kg biochanin A) could relieve the acquisition of adherent and rolling leukocytes (rolling leukocytes:  $30.87 \pm 15.67$  cell/mm<sup>2</sup>,  $27.47 \pm 14.32$  cell/mm<sup>2</sup>,  $20.15 \pm 13.22$  cell/mm<sup>2</sup>, respectively,  $p < 0.01$ , adhering leukocytes:  $4.17 \pm 3.12$  cell/mm<sup>2</sup>,  $3.67 \pm 3.45$  cell/mm<sup>2</sup>,  $2.76 \pm 2.78$  cell/mm<sup>2</sup>,  $p < 0.01$ , Fig. 2B).

### *Biochanin A-mediated attenuation of cerebral blood flow and vascular injury induced by ischemia-reperfusion*

Cerebral blood flow was measured by LDF (FLPI2, Moor, UK). Decreased blood flow was observed during the ischemia-reperfusion operation, and biochanin A could elevate the flow (Fig. 3A). The permeability of the cerebral venule was measured by injecting FITC-labeled albumin through the femoral vein. Based on the statistical data of fluorescence intensity, the ratio of fluorescence intensity of lumen of selected venules (Iv) to that of surrounding interstitial area (Ii) in the same area decreased after ischemia-reperfusion operation (Ii: MCAO/R:  $23435 \pm 478.45$  integral optical density (IOD), sham:  $9765 \pm 207.76$  IOD; Iv: MCAO/R:  $34653 \pm 312.87$  IOD, sham:  $28791 \pm 308.77$  IOD; Ii/Iv: MCAO/R: 67.62%, sham: 33.92%), indicating the vascular damage led to the higher permeability (Fig. 3B). The possible cause is the destruction of vascular basement membrane by peroxides and proteases released by adherent leukocytes and the combined action of inflammatory factors such as histamine. Biochanin A could reduce the proportion of fluorescent leakage in a dose-dependent manner. Different dosages of biochanin A attenuated this leakage and significantly decreased the proportion of fluorescent leakage to lower than that in the cerebral ischemia-reperfusion group (Ii/Iv: 5 mg/kg BA, 52.79%, 10 mg/kg BA, 45.65%, 20 mg/kg BA, 37.14%, Fig. 3B). Tight junctions were continuous and well organized in the sham group, whereas after being stimulated with ischemia-reperfusion, occludin, claudin-5, and ZO-1 revealed structural failure with rearrangements (Fig. 3C). This linear morphology along the junctions was reduced after cerebral ischemia stroke compared to that in the sham-operated group, and the junctions were less pronounced, with weaker intensity and volume of tight junctions (Fig. 3C). After the intervention of biochanin A, the immunocytochemical staining of tight junction protein fragments in the ischemia-reperfusion area improved, and the morphology was clearer and brighter.

Biochanin A dose-dependently ameliorated brain damage in ischemia-reperfusion mice (occludin:  $1.02 \pm 0.17$ , claudin-5:  $1.06 \pm 0.17$ , and ZO-1:  $1.02 \pm 0.13$ ) by strengthening the signal intensity and expression of occludin, claudin-5, and ZO-1 (for occludin: 5 mg/kg, 10 mg/kg, 20 mg/kg biochanin A, and 10 mg/kg nimodipine, respectively:  $1.33 \pm 0.15$ ,  $p < 0.01$ ;  $1.42 \pm 0.16$ ,  $p < 0.01$ ;  $1.49 \pm 0.15$ ,  $p < 0.01$ ;  $1.50 \pm 0.14$ ,  $p < 0.01$ ; claudin-5: 5 mg/kg, 10 mg/kg, 20 mg/kg biochanin A, and 10 mg/kg nimodipine, respectively:  $1.38 \pm 0.18$ ,  $p < 0.01$ ;  $1.43 \pm 0.18$ ,  $p < 0.01$ ;  $1.50 \pm 0.15$ ,  $p < 0.01$ ;  $1.53 \pm 0.15$ ,  $p < 0.01$ ; ZO-1: 5 mg/kg, 10 mg/kg, 20 mg/kg biochanin A, and 10 mg/kg nimodipine, respectively:  $1.29 \pm 0.11$ ,  $p < 0.01$ ;  $1.37 \pm 0.11$ ,  $p < 0.01$ ;  $1.46 \pm 0.18$ ,  $p < 0.01$ ;  $1.44 \pm 0.18$ ,  $p < 0.01$ ) (Fig. 4).

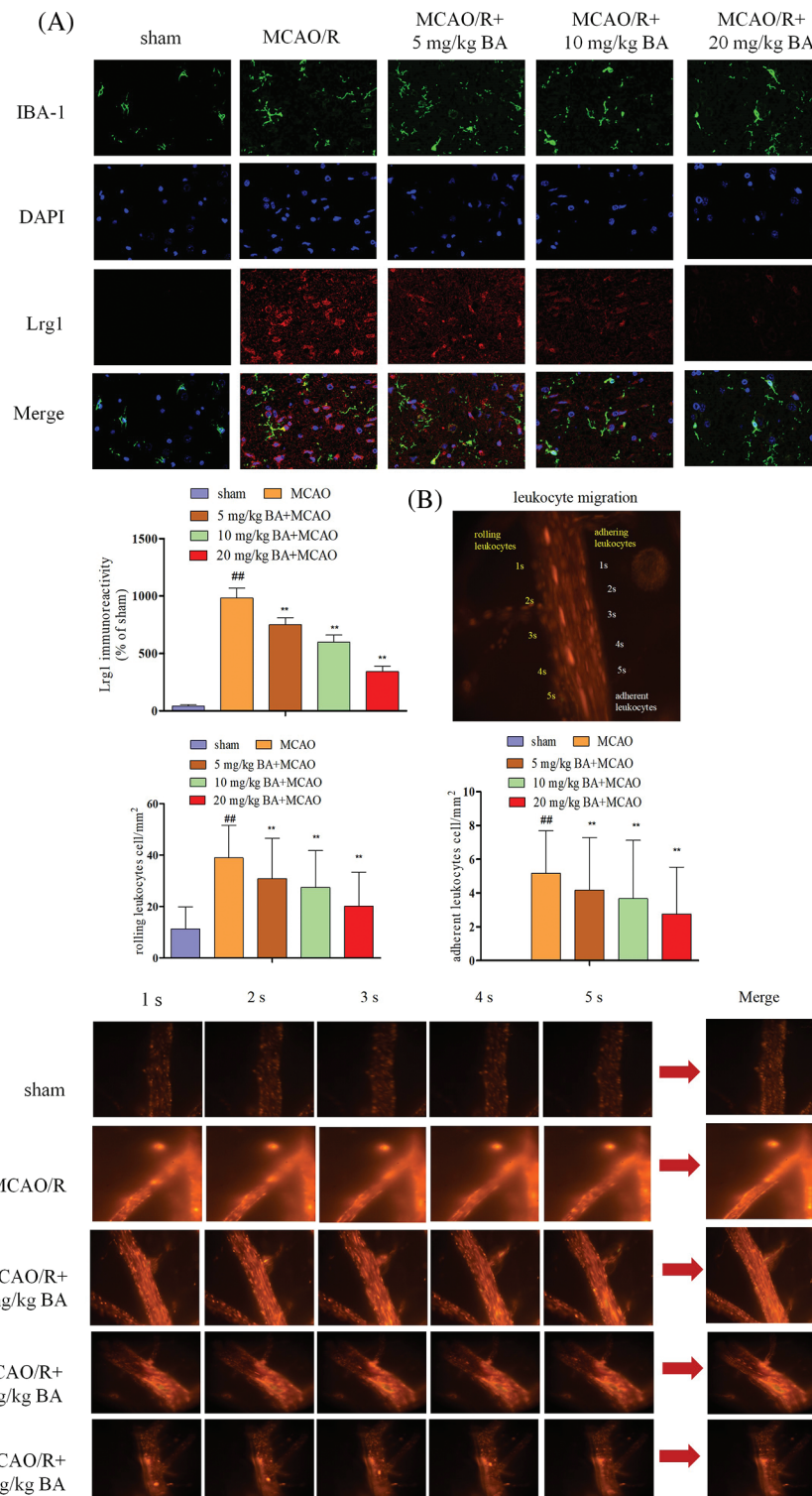


**FIGURE 2.** Biochanin A could inhibit Lrg1 activation and leukocyte migration induced by ischemia-reperfusion. (A) Immunofluorescence staining for microglia (IBA-1, green), Lrg1 (red), and cell nucleus (blue) at 1 h of ischemia and 24 h of reperfusion. Bar = 50  $\mu$ m. (B) Two-photon imaging to analyze the rolling and adhering leukocytes in living mice following ischemia-reperfusion. Rhodamine 6G-stained leukocytes rolled and adhered to cortical vessels (diameter 20–40  $\mu$ m, depth 100–150  $\mu$ m). The view was measured at  $\times 400$  magnification. The figure represents five overlapping images obtained from the first 5 s of the monitoring video. Quantitative measurements of firmly adhering and rolling leukocytes (red). Adherent leukocyte cells ( $\text{mm}^2/\text{vascular surface area}$ ) were counted from at least six fields of view. The values are presented as means  $\pm$  SD,  $n = 8$ , <sup>##</sup> $p < 0.01$  vs. sham mice, <sup>\*\*</sup> $p < 0.01$  vs. ischemia-reperfusion mice.

The expression of Lrg1, TGF- $\beta$ 1, and the phosphorylation of Smad2/Smad2 also increased (Lrg1:  $1.69 \pm 0.17$ ,  $p < 0.01$ ; TGF- $\beta$ 1:  $1.67 \pm 0.10$ ,  $p < 0.01$ ; p-Smad2/Smad2:  $1.63 \pm 0.10$ ,  $p < 0.01$ ) in accordance with the alternation of the tight

junction. The data showed that biochanin A ameliorated the pathological damage of brain tissues by enhancing the immunostaining signal intensity of occludin, claudin-5, and ZO-1, whereas the upregulation of Lrg1, TGF- $\beta$ 1, and the

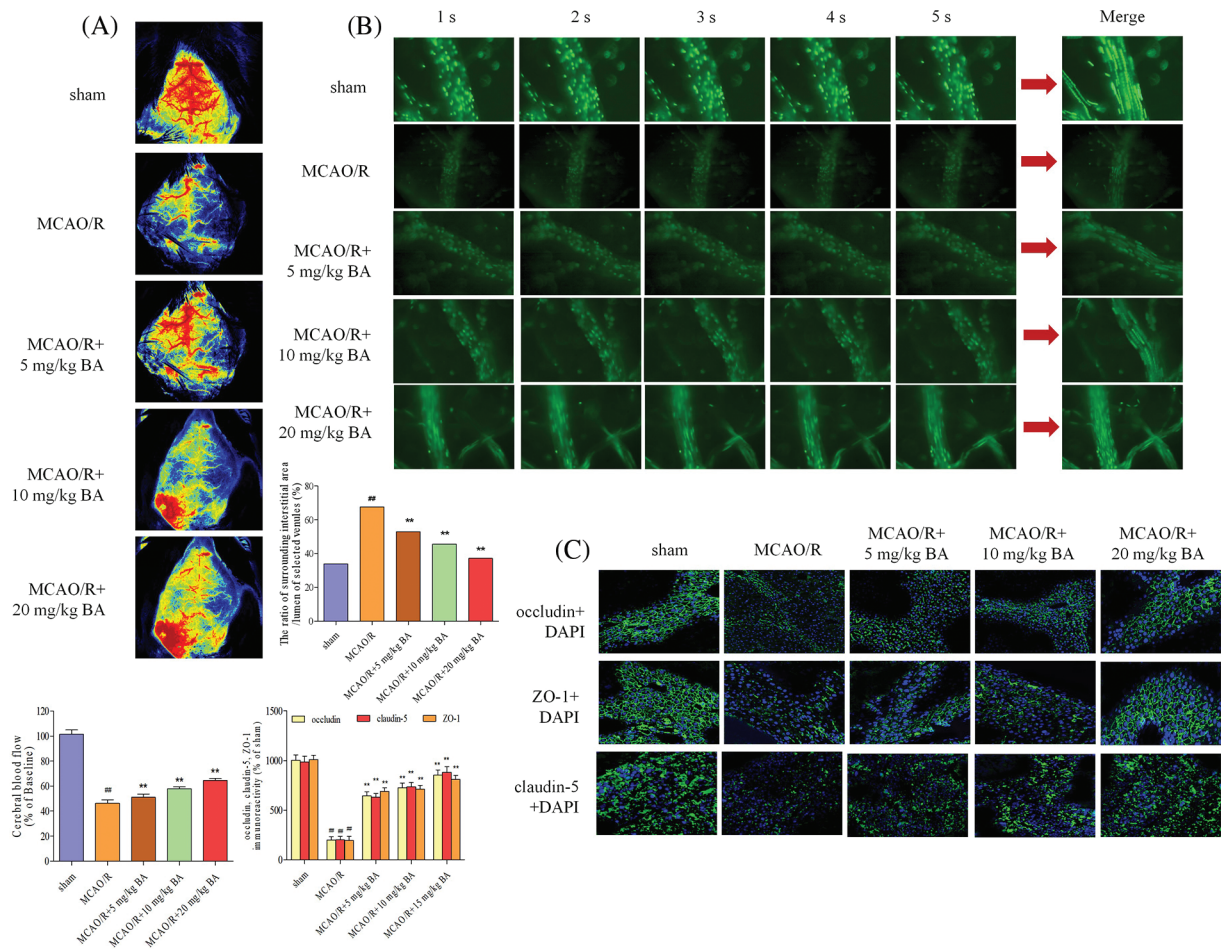


**FIGURE 3.** Biochanin A could attenuate cerebral blood flow and vascular injury induced by ischemia-reperfusion. (A) Cerebral blood flow was measured under a laser Doppler flowmetry. Mice detected with the decrease in the middle cerebral artery blood flow to less than 30% of the basic flow were discarded during the experimentation. (B) The permeability of the cerebral venule was measured by injecting fluorescein isothiocyanate-labeled albumin through the femoral vein. The changes in venular permeability were quantified with the ratio of the fluorescence intensity in and out of the venules. Data were expressed as integral optical density, while the ratio of fluorescence intensity of the lumen of selected venules (Iv) to that of the surrounding interstitial area (Ii) was expressed as %. The figure represents five overlapping images obtained from the first 5 s of the monitoring video of each group. The observation view was measured under  $\times 400$  magnified. (C) Effects of biochanin A on immunofluorescence changes in the tight junction exposed to 1 h of ischemia and 24 h of reperfusion. Immunofluorescence staining for the tight junction proteins occludin, claudin-5, and ZO-1 (green). The images represent six individual areas from each group. Bar = 50  $\mu$ m.

phosphorylation of Smad2/Smad2 were inhibited (Lrg1: 5 mg/kg, 10 mg/kg, 20 mg/kg biochanin A, and 10 mg/kg nimodipine, respectively:  $1.60 \pm 0.17$ ,  $p < 0.01$ ;  $1.45 \pm 0.13$ ,  $p < 0.01$ ;  $1.34 \pm 0.14$ ,  $p < 0.01$ ;  $1.33 \pm 0.17$ ,  $p < 0.01$ ; TGF- $\beta$ 1: 5 mg/kg, 10 mg/kg, 20 mg/kg biochanin A, and 10 mg/kg nimodipine, respectively:  $1.55 \pm 0.12$ ,  $p < 0.01$ ;  $1.42 \pm 0.12$ ,  $p < 0.01$ ;  $1.33 \pm 0.10$ ,  $p < 0.01$ ;  $1.35 \pm 0.14$ ,  $p < 0.01$ ; p-Smad2/Smad2: 5 mg/kg, 10 mg/kg, 20 mg/kg biochanin A, and 10 mg/kg nimodipine, respectively:  $1.60 \pm 0.13$ ,  $p < 0.05$ ;  $1.46 \pm 0.13$ ,  $p < 0.01$ ;  $1.35 \pm 0.15$ ,  $p < 0.01$ ;  $1.33 \pm 0.16$ ,  $p < 0.01$ ) (Fig. 4).

*The function of biochanin A in alleviating the blood-brain barrier permeability and infarct volume on conventional Lrg1-knockout mice*

Lrg1-KO mice presented undifferentiated EB leakage and infarct volume (sham+WT:  $0.12 \pm 0.09$ ) compared with those of WT (sham+KO:  $0.15 \pm 0.07$ ) mice under sham operation condition (Fig. 5A). Less extensive EB leakage in

the ischemia brain were observed in Lrg1-KO mice after ischemia-reperfusion (MCAO/R+WT:  $2.65 \pm 0.05$ ,  $p < 0.01$ , MCAO/R+KO:  $1.46 \pm 0.11$ ,  $p < 0.01$ , Fig. 5A), while much smaller infarct volume (MCAO/R+WT:  $47.33 \pm 2.09$ ,  $p < 0.01$ , MCAO/R+KO:  $23.75 \pm 2.45$ ,  $p < 0.01$ ) were observed under ischemia-reperfusion condition (Fig. 5B). The attenuated effects of Lrg1-KO mice on tight junction injury (EB leakage: MCAO/R+KO:  $1.46 \pm 0.11$ , MCAO/R+KO+biochanin A:  $1.47 \pm 0.13$ ; infarct volume: MCAO/R+KO:  $23.75 \pm 2.45$ , MCAO/R+KO+biochanin A:  $24.87 \pm 2.46$ ) were approximately in agreement with the intervention functions of biochanin A. Biochanin A could not improve continued attenuation for tight junction injury on Lrg1-KO mice under ischemia-reperfusion condition. Immunohistochemical assessment for tight junction proteins occludin, claudin-5, and ZO-1 more continuity was retained and intensified in Lrg1-KO mice compared with those in WT mice after ischemia-reperfusion (Fig. 5C).

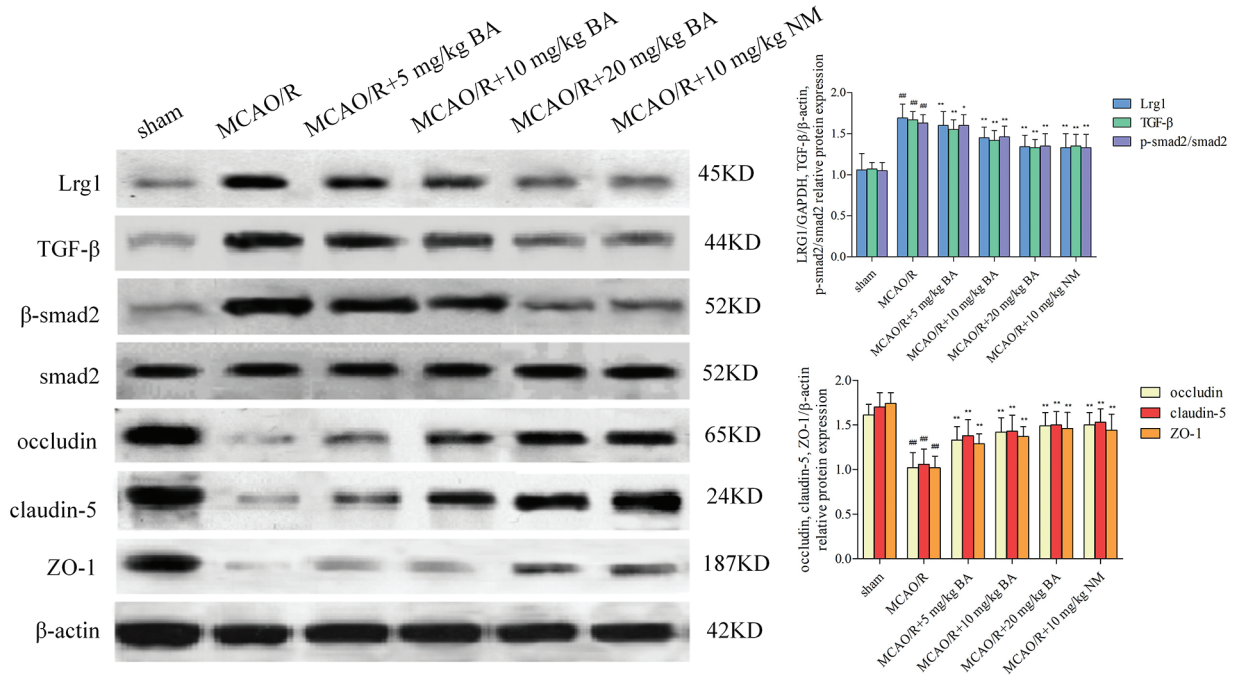


**FIGURE 4.** Western blotting to determine the effects of biochanin A on the tight junction proteins and Lrg1, TGF-β1, and p-Smad2/Smad2 in ischemia-reperfusion mice. Nimodipine (10 mg/kg) was administrated as the positive control. Results represent eight independent experiments, and the data are represented as the mean ± SD, n = 8. ##*p* < 0.01 vs. sham mice, \**p* < 0.05, \*\**p* < 0.01 vs. ischemia-reperfusion mice. Sham, sham-operated mice; MCAO, mice exposed to 1 h of ischemia and 24 h of reperfusion; BA, mice treated with biochanin A; NM, mice treated with nimodipine.

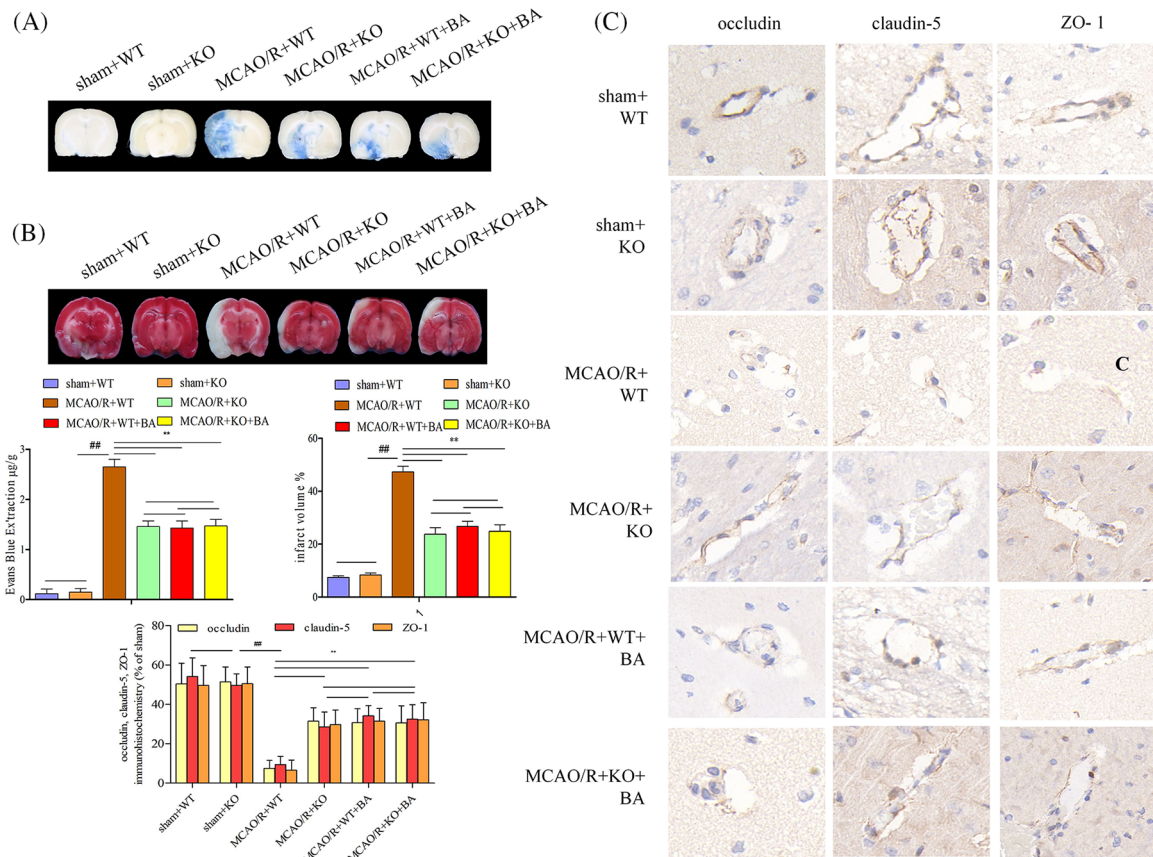


**FIGURE 5.** The function of biochanin A on the alleviation of blood-brain barrier permeability and infarct volume in conventional Lrg1-knockout mice. (A) Representative gross appearance and quantitative analysis of Evans blue-stained brains exposed to 1 h of ischemia and 24 h of reperfusion. (B) Representative cerebral tissues and quantitative analysis of TTC stained brains subjected to 1 h of ischemia and 24 h of reperfusion. (C) Immunohistochemical staining of occludin, claudin-5, and ZO-1 for brain tissues exposed to 1 h of ischemia and 24 h of reperfusion. Bar = 20 μm. Results included eight independent experiments, and the data represented the mean ± S.D., n = 8. ##*p* < 0.01 vs. sham WT mice, \*\**p* < 0.01 vs. ischemia-reperfusion WT mice.

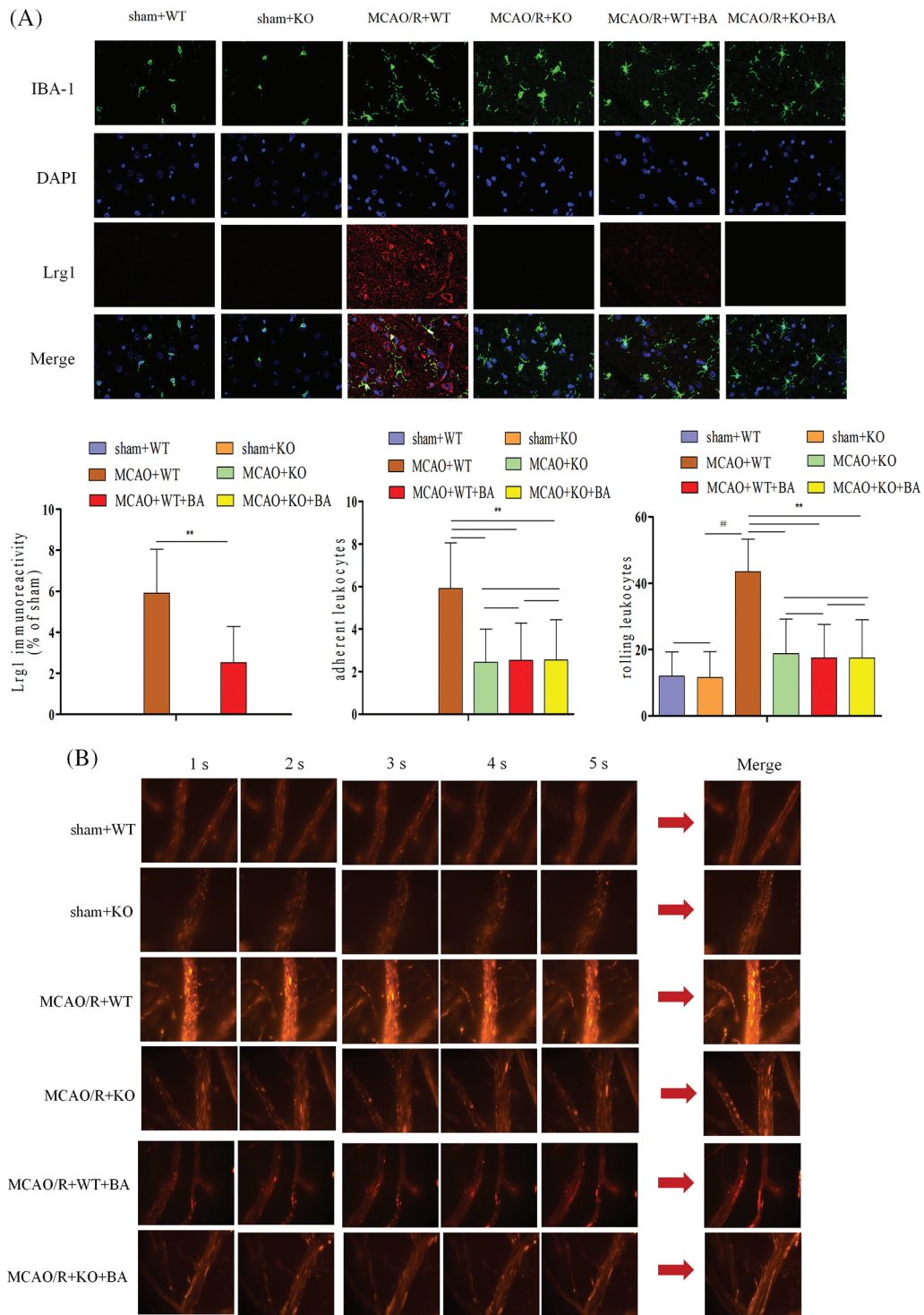


**FIGURE 6.** The function of biochanin A on the microglia activation and leukocyte migration on conventional Lrg1-knockout mice. (A) Immunofluorescence staining for microglia (IBA-1, green), Lrg1 (red), and cell nucleus (blue) after 1 h of ischemia and 24 h of reperfusion mice. Bar = 50  $\mu$ m. (B) Two-photon imaging to analyze the adherent and rolling leukocytes in living mice following ischemia-reperfusion. Cortical vessels (diameter 20–40  $\mu$ m, depth 100–150  $\mu$ m) were observed for imaging via two-photon imaging. Rhodamine 6G-labeled leukocytes were visualized for adherence and rolling in the vessel at 1 h of ischemia and 24 h of reperfusion. The observation view was measured under  $\times 400$  magnified view. The figure represents five overlapping images obtained from the first 5 s monitoring video. Firmly adherent and rolling leukocytes (red) were quantitatively measured. Adherent leukocytes cells ( $\text{mm}^2/\text{vascular surface area}$ ) were counted from at least six fields of view, means  $\pm$  S.D.,  $n = 8$ ,  $^{##}p < 0.01$  vs. sham WT mice,  $^{**}p < 0.01$  vs. ischemia-reperfusion wild-type (WT) mice.

*The function of biochanin A on the microglia activation and leukocyte migration in conventional Lrg1-knockout mice*  
 After the stimulation of ischemia-reperfusion in Lrg1-KO mice, microglia presented deactivation with a less

amoeba-like form. Biochanin A could not suppress the elevation of Lrg1 fluorescent intensity on ischemia-reperfusion Lrg1-KO mice (Fig. 6A). Adhering leukocytes and rolling leukocytes presented less fluorescent staining in

Lrg1-KO mice after the stimulation of ischemia-reperfusion compared with that of WT mice (Fig. 6B). Also, a significant decrease in the rolling velocity of rolling leukocytes was detected in the Lrg1-KO brain vessels of ischemia-reperfusion mice (MCAO/R+WT:  $43.50 \pm 5.76$ , MCAO/R+KO:  $24.87 \pm 2.46$ ,  $p < 0.01$ ; Fig. 6B). Biochanin A could not further relieve the acquisition of adhering and rolling leukocytes in Lrg1-KO mice compared with that of Lrg1-KO mice after ischemia-reperfusion (adhering leukocytes: MCAO/R+KO:  $2.44 \pm 1.56$ , MCAO/R+KO+biochanin A:  $1.76 \pm 2.55$ ; rolling leukocytes: MCAO/R+KO:  $18.77 \pm 10.45$ , MCAO/R+KO+biochanin A:  $17.55 \pm 11.46$ ; Fig. 6B).

*The function of biochanin A on the cerebral blood flow and vascular injury in conventional Lrg1-knockout mice*

Cerebral blood flow increased in conventional Lrg1-KO mice during the ischemia-reperfusion operation (Fig. 7A). The cerebral venular permeability was also relieved in conventional Lrg1-KO mice compared with that in WT mice treated with ischemia-reperfusion (Fig. 7B). The ratio of fluorescence intensity of the lumen of selected venules (Iv) to surrounding interstitial area (Ii) of FITC-labeled albumin was decreased in conventional Lrg1-KO mice under ischemia-reperfusion (Ii: MCAO/R+KO:  $16477 \pm 386.32$  OD, MCAO/R+WT:  $25693 \pm 223.87$  OD; Iv: MCAO/R+KO:  $36323 \pm 267.83$  OD, MCAO/R+WT:  $36877 \pm 307.23$

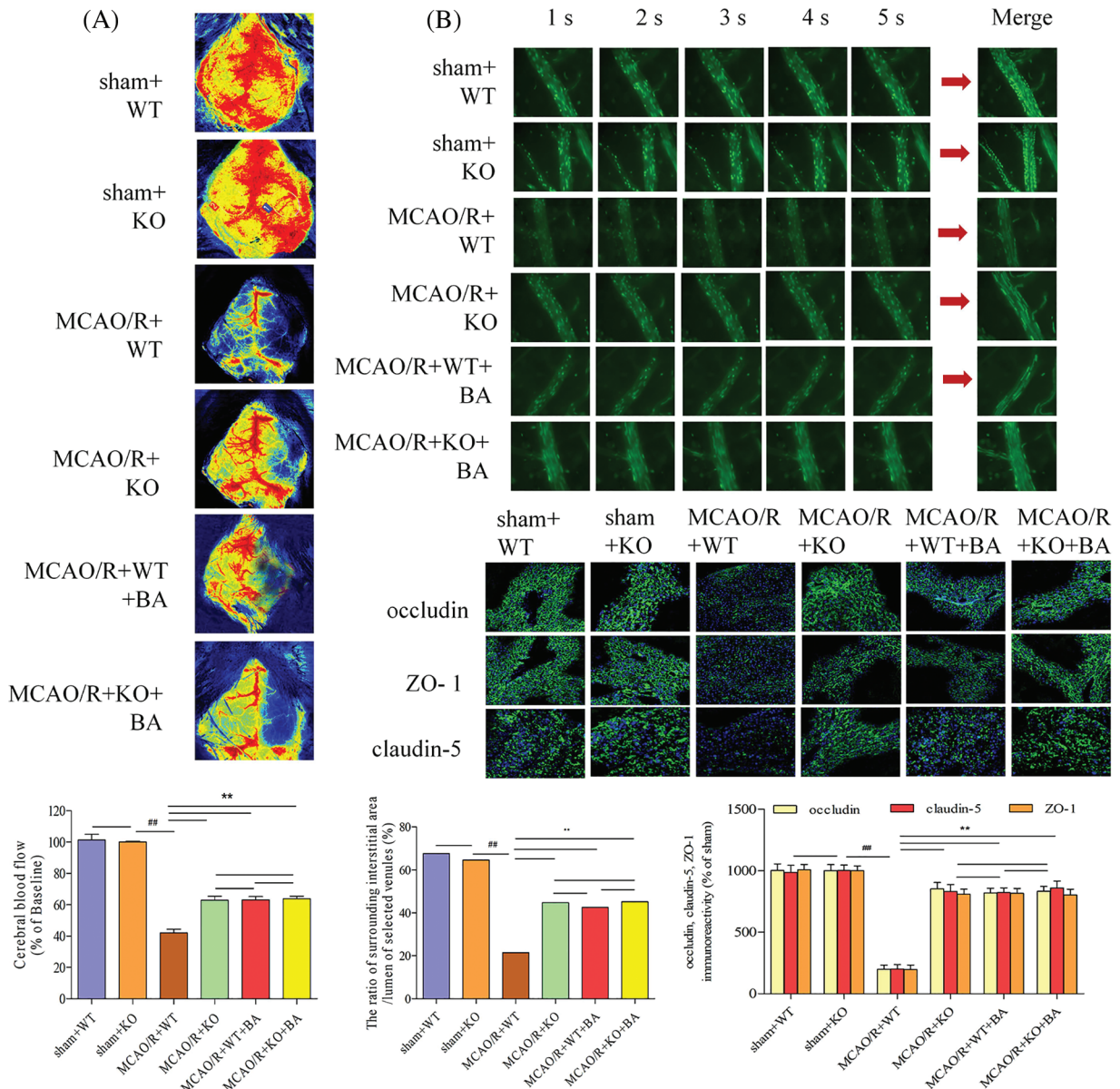


**FIGURE 7.** The function of biochanin A on cerebral blood flow and vascular injury in conventional Lrg1-knockout mice. (A) Cerebral blood flow was measured under a laser Doppler flowmetry. The mice detected with the decrease in the middle cerebral artery blood flow below 30% of the basic flow were discarded during the experimental operation. (B) Biochanin A treatment on fluorescein isothiocyanate-labeled albumin from small veins. The changes in venular permeability were quantified with the ratio of the fluorescence intensity in and out of the venules. The observation was measured under  $\times 400$  magnification. The figure represents five overlapping images obtained from the first 5 s of the monitoring video. Data were expressed as means  $\pm$  SD.  $n = 8$ ,  $##p < 0.01$  vs. sham WT mice,  $**p < 0.01$  vs. ischemia-reperfusion WT mice. (C) Effects of biochanin A on immunofluorescence changes in the tight junction exposed to 1 h of ischemia and 24 h of reperfusion mice. Immunofluorescence staining for the tight junction proteins occludin, claudin-5, and ZO-1 (green). The images were representative of eight individual areas from each group. Bar = 50  $\mu$ m.

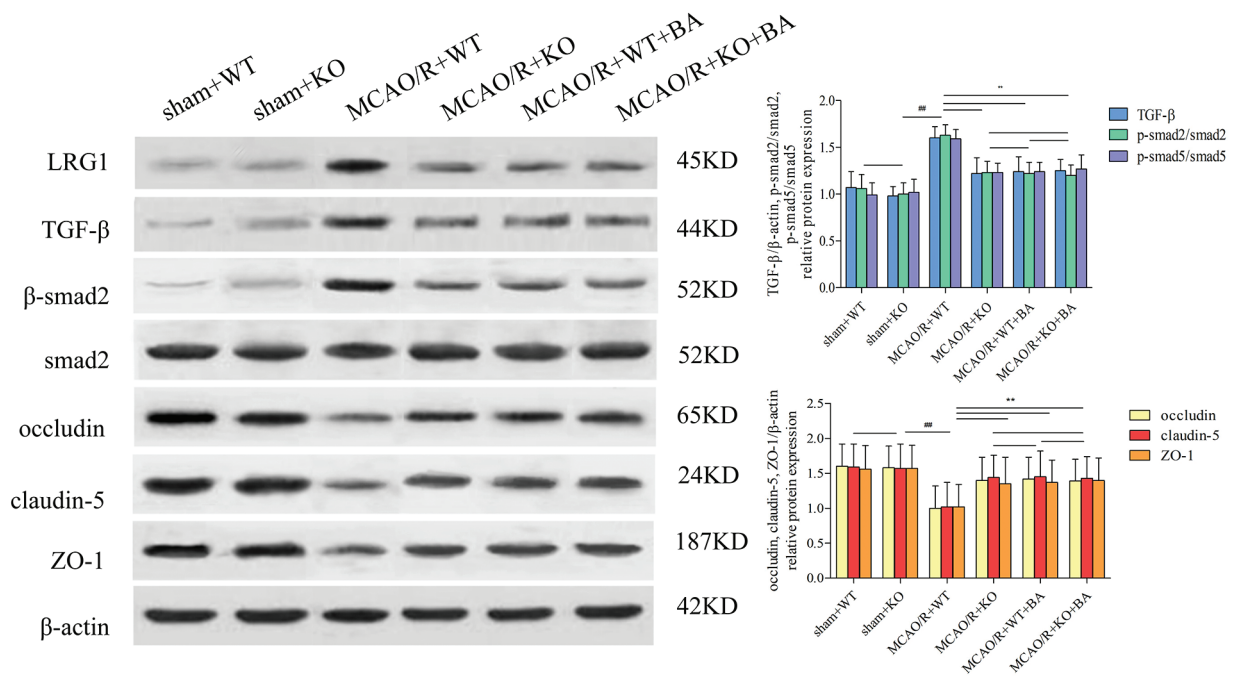


**FIGURE 8.** The function of biochanin A on tight junction protein and Lrg1, TGF-β1, and phosphorylated (p)-Smad2/Smad2 in conventional Lrg1-knockout (Lrg1-KO) mice after ischemia-reperfusion by western blotting. Results represent six independent experiments, and the data are presented as mean ± SD, n = 8. <sup>#</sup>*p* < 0.01 vs. sham WT mice, <sup>\*\*</sup>*p* < 0.01 vs. ischemia-reperfusion WT mice.

OD; Ii/Iv: MCAO/R+KO: 45.36%, sham: 69.67%, Fig. 7B). The treatment of biochanin A had no influence on the Ii/Iv ratio of FITC-labeled albumin on conventional Lrg1-KO ischemia-reperfusion mice (Ii: MCAO/R+KO+biochanin A: 15976 ± 317.45 OD; Iv: 37488 ± 330.24 OD; Ii/Iv: MCAO/R+KO+biochanin A: 42.62%). Occludin, claudin-5, and ZO-1 were more well organized in conventional Lrg1-KO mice compared with that in the WT group after ischemia-reperfusion. Biochanin A could not exert structural re-arrangements on the tight junction in conventional Lrg1-KO ischemia-reperfusion mice (Fig. 7C).

The attenuated effects of conventional knockout Lrg1 on tight junction injury (MCAO/R+KO: occludin: 1.40 ± 0.33, *p* < 0.01; claudin-5: 1.44 ± 0.32, *p* < 0.01; ZO-1: 1.35 ± 0.38, *p* < 0.01; Fig. 8) were approximately in agreement with the intervention functions of biochanin A (MCAO/R+KO+biochanin A: occludin: 1.39 ± 0.31, *p* < 0.01; claudin-5: 1.43 ± 0.31, *p* < 0.01; ZO-1: 1.40 ± 0.32, *p* < 0.01; Fig. 8). Biochanin A could not improve continued attenuation for tight junction injury on conventional Lrg1-KO mice under ischemia-reperfusion. Furthermore, Lrg1, TGF-β1, and Smad2/Smad2 phosphorylation were also inhibited in conventional Lrg1-KO mice. Lrg1 might be the key factor necessary to form a tight junction of BBB, whereas biochanin A exerted its functions through the regulation of Lrg1.

**Discussion**

Biochanin A is an oxymethylated isoflavone compound that is widely found in some edible plants, such as soybean, red clover, alfalfa, peanut, chickpea, etc. The molecular structure of biochanin A is similar to that of estrogen, and it can competitively bind to estrogen receptors and exert

estrogen-like effects. The multiple functions of biochanin A include anti-inflammatory, neuroprotective, and antimicrobial properties. More importantly (Sarfranz et al., 2020; Zarmouh et al., 2017), biochanin A is an excellent dietary isoflavone that has the concomitant function of both medicine and foodstuff. The metabolism of biochanin A was characterized *in vivo* through Uhlpc-Q-Tof-Ms/Ms methods (Yin et al., 2019). Also, biochanin A was identified as a special cleaving enzyme 1 inhibitor (Youn et al., 2016), and as a nutritional supplementation for the amelioration of PM 2.5-induced lung toxicity (Xue et al., 2020). However, besides this study, few others have shown that biochanin A interventions counteract the pathological process of ischemia-reperfusion. Only some experimental reports stated that biochanin A protects the ischemic brain from oxidative and inflammatory effects via the nuclear factor erythroid 2 related factor 2 and nuclear factor-kappa beta (NF-κB) pathway (Guo et al., 2019). Glutamate excitotoxic contributes to neuronal cell death after ischemia stroke, while biochanin A attenuates stroke by decreasing the expression of glutamate oxaloacetate transaminase in the brain tissues (Khanna et al., 2017). In another study, biochanin A alleviated cerebral ischemia-reperfusion damage through the inhibition of cellular apoptosis induced by endoplasmic reticulum stress (Guo et al., 2021). Additionally, biochanin A has been reported to act on neuro-related diseases. Biochanin A exerted protective effects in angiotensin II-induced model rats through the regulation of Eph receptor A2 and angiotensin II type 1 receptor (Xue et al., 2019). Furthermore, biochanin A might provide neuroprotection against subarachnoid hemorrhage by blocking the action of inflammatory injury through the toll-like receptor/TIR domain-containing adapter protein/myeloid differentiation factor88/NF-κB signaling pathway

(Wu *et al.*, 2018). Biochanin A could selectively reverse monoamine oxidase B in the pathological process of Parkinson’s and Alzheimer’s diseases (Nakajima *et al.*, 2012). In this study, biochanin A could relieve the BBB leakage and reduce the infarct volume of ischemic stroke mice. Stroke is the most common chronic disease among middle-aged and older people. For its safety and effectiveness, biochanin A could act as long-term complementary nutritional supplementation for ischemic stroke (Fig. 9).

Lrg1 is a member of the large family of leucine-rich repeat, with the molecular weight of mature protein being 45 kDa. The vast majority of leucine-rich repeat proteins that have been highly expressed in the nervous system are transmembrane proteins, which participate in normal physiological activities of the nervous system, such as synapse formation, neural growth, and neurotransmitters release as cell adhesion molecules (Zou *et al.*, 2022). A variety of proteins in the nervous system have a leucine-rich repeat structure. In some neurodegenerative diseases, such as the cerebrospinal fluid of Alzheimer’s disease patients, Lrg1 expression was more highly concentrated than in healthy old individuals (Zheng *et al.*, 2019; Xu *et al.*, 2021). Compared with normal patients, the expression of Lrg1 in cerebrospinal fluid of patients with idiopathic normal pressure hydrocephalus exhibited a specific increase (Nakajima *et al.*, 2012). There have been a few experimental reports on Lrg1 and ischemic stroke. Serum Lrg1 is a diagnostic and prognostic index for the degree and progression of stroke (Zhang *et al.*, 2021). Lrg1 also exacerbates ischemia-reperfusion injury by promoting apoptosis and autophagy by regulating the TGF- $\beta$ -smad1/5 signaling pathway (Jin *et al.*, 2019). Overexpression of Lrg1

aggravates cerebral infarction in ischemia rats, enhancing apoptosis and autophagy in brain tissue (Yamashita *et al.*, 2010). In the ischemia mouse model, Lrg1 promoted endothelial cell mitosis and angiogenesis via the activation of the TGF- $\beta$  pathway (Meng *et al.*, 2016; Cao *et al.*, 2020; Pek *et al.*, 2015). Lrg1 is also closely related to lipid metabolism, and its expression could be upregulated in early atherosclerosis, increasing the occurrence of atherosclerosis and vascular endothelial dysfunction (Xu *et al.*, 2021; Nakajima *et al.*, 2012). However, the specific molecular mechanism of the action of Lrg1 in the BBB or tight junction injury induced by ischemia-reperfusion and the specific intervention drugs on Lrg1 are little known.

Tight junction proteins located in endothelial cells comprise a hallmark of the BBB (Lv *et al.*, 2019). The tight junction suffered from damage, such as cerebral ischemia or trauma. When the tight junction suffered from ischemia-reperfusion, tight junction protein was characterized by various morphological changes, simultaneously with the loss of occludin, claudin-5, and ZO-1. Microglial and astrocytic activation induced BBB injury after ischemia-reperfusion by reducing inflammation (Liu *et al.*, 2020). Reports have elucidated that the depletion of microglia leads to leukocyte infiltration in the ischemia brain (Otxoa-de-Amezaga *et al.*, 2019; Jin *et al.*, 2017). Microglial-mediated inflammatory factors increase cerebrovascular permeability during ischemic stroke (Su *et al.*, 2017). Whereas the mechanism of entry of leukocytes admitted into the vessel induced by microglial had not been clarified. Here, under the live view of ischemia-reperfusion mice brain, rolling and adherent leukocytes were evaluated by counting for a limited time. Chemokines are important in regulating leukocyte aggregation, whereas the role of the chemokine CXCL was

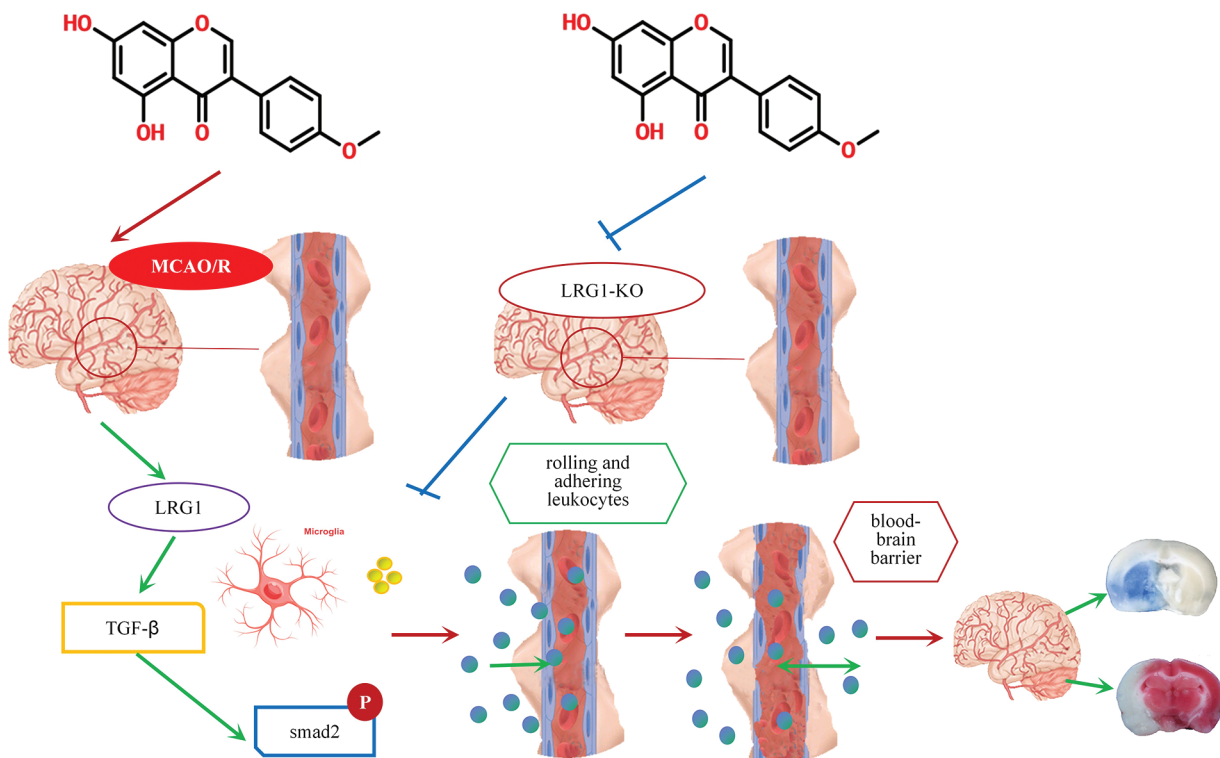


FIGURE 9. A schematic diagram of the role of biochanin A as a long-term complementary nutritional supplementation for ischemic stroke.

limited. CXCL13 mediated the inhibition of microglial activation in the spinal cord (Li *et al.*, 2017), while CXCL10 regulated the M1/M2 Macrophage polarization and oxidative/antioxidative biochanin Alance (Tsai *et al.*, 2021). Our research showed under the living brain view, the rolling rate and an aggregative number of leukocytes were elevated during the ischemia-reperfusion. The migration speed and number of leukocytes were consistent with the morphologic change of microglia. Biochanin A might inhibit the activation of microglia for the prevention of neuroinflammation and oxidative stress (Berköz *et al.*, 2020; Wu *et al.*, 2015). Here, biochanin A could attenuate tight junction injury via the downregulation of Lrg1, while biochanin A could not exert further attenuation effects on conventional Lrg1-KO mice. Biochanin A, as the Lrg1 blockade, participated in reducing the damage to the BBB damage induced by ischemia-reperfusion injury.

A few reports are available on the relationship between Lrg1 and the tight junction. Existing studies have shown that Lrg1 could regulate the TGF- $\beta$  signaling pathway, whereas TGF- $\beta$  has been reported to be associated with variation in the tight junction. TGF- $\beta$ 1-mediated exosomal lnc-matrix metalloproteinase 2-2 promotes non-small cell lung cancer brain metastasis by increasing the permeability of the BBB (Wu *et al.*, 2021). Methylmercury up-regulated the expression of TGF- $\beta$  mRNA in the cerebellum of rats, damaging the BBB and causing neurobehavioral changes (Abu-Zeid *et al.*, 2021). Platelet-derived growth factor receptor- $\alpha$  effects might be mediated by TGF- $\beta$ 1, which exerts potent protective effects on the BBB (Nguyen *et al.*, 2021). Also, Smad2 might be involved in the pathological process of ischemic stroke. Stem cell-derived small extracellular vesicles induced a sharp rise in the regulatory T cells, and this process is dependent on the activation of the TGF- $\beta$ /smad signaling pathway (Xia *et al.*, 2021). BBB integrity suffered and was destroyed at 12 h and 24 h after MCAO, and the levels of TGF- $\beta$ 1, TGF- $\beta$ R(II), and p-Smad2/3 were upregulated (Yang *et al.*, 2021). In this study, we found that biochanin A might specifically target Lrg1. Lrg1 was upregulated on ischemia-reperfusion mice, accompanied with TGF- $\beta$ 1 activation and Smad2 phosphorylation. In Lrg1 knockdown endothelial cells, TGF- $\beta$ 1 and Smad2 phosphorylation could not be upregulated by stimulated ischemia-reperfusion. Biochanin A could attenuate tight junction injury via Lrg1 downregulation, inhibition of TGF- $\beta$ 1 activation and Smad2 phosphorylation. Additionally, in ischemia-reperfusion conventional Lrg1-KO mice, biochanin A could not further attenuate the regulation of Lrg1, TGF- $\beta$ 1, and Smad2 phosphorylation.

### Limitations

In the measurement of FITC-labeled albumin fluorescence intensity, in some cases, the blood flow stopped due to microcirculation disorders, which blocked the flow of albumin macromolecules into the blood vessels, resulting in extremely low intravascular fluorescence intensity. The vessels with low baseline fluorescence of sham operation

mice were excluded, and this did not affect the data statistics of fluorescence.

### Conclusions

The exploitation of biochanin A could be identified as a concomitant function of both medicine and food during chronic disease, like ischemia-reperfusion. On the microscope observation of living mice, biochanin A could play a countervailing role in the accumulation of rolling and adherence of leukocytes to the vessel. The amoeba-like change in microglial morphology was consistent with Lrg1 upregulation, which was attenuated by biochanin A treatment. The inflammatory damage induced an increase in the ratio of fluorescence intensity of the interstitial area to lumen venule, which was reduced after biochanin A treatment, accompanied by the attenuation of continuity and integrity of tight junction proteins. Biochanin A diminished its functions to further improve attenuation for tight junction injury in conventional Lrg1-KO mice and the inhibition effects on the expression of TGF- $\beta$ 1 and the phosphorylation of Smad2/Smad2. In conclusion, biochanin A could alleviate tight junction injury induced by cerebral ischemia-reperfusion, while acting to block the Lrg1/TGF- $\beta$ /Smad2 pathway to modulate leukocyte migration patterns.

**Acknowledgement:** Key Laboratory of Modern Preparation of TCM of Jiangxi University of Traditional Chinese Medicine helped to provide immunofluorescence experimental assay.

**Funding Statement:** This work was supported by a Foundation Project: National Natural Science Foundation of China (Nos. 82100417, 81760094), China; The Foundation of Jiangxi Provincial Department of Science and Technology Project (Nos. 20202ACBL206001, 20212BAB206022, 20181BAB205026). The funder had no role in the study design, data collection, analysis, or the decision to publish or prepare the manuscript.

**Author Contributions:** Longsheng Fu wrote the main manuscript text, analyzed the main data, prepared all the figures, and reviewed the manuscript. Jinfang Hu wrote the main manuscript, analyzed the data, and reviewed the manuscript. Feng Shao designed the experiment, wrote the main manuscript text, and reviewed the manuscript. Yaoqi Wu analyzed the main data, prepared all the figures, and reviewed the manuscript. Wei Bai analyzed the main data, prepared all the figures, and reviewed the manuscript; Mingjin Jiang analyzed the main data, prepared all the figures, and reviewed the manuscript. Hao Chen analyzed the main data, prepared all the figures, and reviewed the manuscript. Lihua Chen designed the experiment, wrote the main manuscript text, and reviewed the manuscript. Yanni Lv designed the experiment, wrote the main manuscript text, and reviewed the manuscript.

**Availability of Data and Materials:** All data generated or analyzed during this study were included in this published article.

**Ethic Approval:** The experimental protocol was established according to the ethical guidelines and was approved by the Ethics Committee of The First Affiliated Hospital of Nanchang University and Nanchang University (No. 202212214).

**Conflicts of Interest:** The authors declare that they have no conflicts of interest to report regarding the present study.

## References

- Abu-Zeid EH, Khalifa BA, Elewa YHA, Arisha AH, Ismail TA, Hendam BM, Abdel-Hamid SE (2021). Bee venom *Apis mellifera lamarckii* rescues blood brain barrier damage and neurobehavioral changes induced by methyl mercury via regulating tight junction proteins expression in rat cerebellum. *Food and Chemical Toxicology* **154**: 112309. <https://doi.org/10.1016/j.fct.2021.112309>
- Berköz M, Krośniak M, Özkan-Yılmaz F, Özlüer-Hunt A (2020). Prophylactic effect of Biochanin A in lipopolysaccharide-stimulated BV2 microglial cells. *Immunopharmacology and Immunotoxicology* **42**: 330–339. <https://doi.org/10.1080/08923973.2020.1769128>
- Cao JW, Zhong D, Li GZ (2020). LRG1 and TGF after cerebral ischemia in mice- $\beta 1$ . *Journal of Brain and Neurological Diseases* **28**.
- Chen B, Sun K, Liu YY, Xu XS, Wang CS, Zhao KS, Huang QB, Han JY (2016). Effect of salvianolic acid B on TNF- $\alpha$  induced cerebral microcirculatory changes in a micro-invasive mouse model. *Chinese Journal of Traumatology = Zhonghua Chuang Shang Za Zhi* **19**: 85–93. <https://doi.org/10.1016/j.cjtee.2015.07.011>
- Guo M, Lu H, Qin J, Qu S, Wang W, Guo Y, Liao W, Song M, Chen J, Wang Y (2019). Biochanin A provides neuroprotection against cerebral ischemia/reperfusion injury by Nrf2-mediated inhibition of oxidative stress and inflammation signaling pathway in rats. *Medical Science Monitor* **25**: 8975–8983. <https://doi.org/10.12659/MSM.918665>
- Guo MM, Qu SB, Lu HL, Wang WB, He ML, Su JL, Chen J, Wang Y (2021). Biochanin A alleviates cerebral ischemia/reperfusion injury by suppressing endoplasmic reticulum stress-induced apoptosis and p38MAPK signaling pathway in vivo and in vitro. *Frontiers in Endocrinology* **12**: 646720. <https://doi.org/10.3389/fendo.2021.646720>
- Jin WN, Shi SX, Li Z, Li M, Wood K, Gonzales RJ, Liu Q (2017). Depletion of microglia exacerbates postischemic inflammation and brain injury. *Journal of Cerebral Blood Flow and Metabolism* **37**: 2224–2236. <https://doi.org/10.1177/0271678X17694185>
- Jin J, Sun H, Liu D, Wang H, Liu Q, Chen H, Zhong D, Li G (2019). LRG1 promotes apoptosis and autophagy through the TGF $\beta$ -smad1/5 signaling pathway to exacerbate ischemia/reperfusion injury. *Neuroscience* **413**: 123–134. <https://doi.org/10.1016/j.neuroscience.2019.06.008>
- Khanna S, Stewart R, Gnyawali S, Harris H, Balch M, Spieldenner J, Sen CK, Rink C (2017). Phytoestrogen isoflavone intervention to engage the neuroprotective effect of glutamate oxaloacetate transaminase against stroke. *FASEB Journal* **31**: 4533–4544. <https://doi.org/10.1096/fj.201700353>
- Li J, Deng G, Wang H, Yang M, Yang R, Li X, Zhang X, Yuan H (2017). Interleukin-1 $\beta$  pre-treated bone marrow stromal cells alleviate neuropathic pain through CCL7-mediated inhibition of microglial activation in the spinal cord. *Scientific Reports* **7**: 42260. <https://doi.org/10.1038/srep42260>
- Liu M, Xu Z, Wang L, Zhang L, Liu Y et al. (2020). Cottonseed oil alleviates ischemic stroke injury by inhibiting the inflammatory activation of microglia and astrocyte. *Journal of Neuroinflammation* **17**: 270.
- Lv YN, Fu LS (2018). The potential mechanism for Hydroxysafflor yellow A attenuating blood-brain barrier dysfunction via tight junction signaling pathways excavated by an integrated serial affinity chromatography and shotgun proteomics analysis approach. *Neurochemistry International* **112**: 38–48.
- Lv Y, Liu W, Ruan Z, Xu Z, Fu L (2019). Myosin IIA regulated tight junction in oxygen glucose-deprived brain endothelial cells via activation of TLR4/PI3K/Akt/JNK1/2/14-3-3 $\epsilon$ /NF- $\kappa$ B/MMP9 signal transduction pathway. *Cellular and Molecular Neurobiology* **39**: 301–319.
- Mendelson SJ, Prabhakaran S (2021). Diagnosis and management of transient ischemic attack and acute ischemic stroke: A review. *The Journal of the American Medical Association* **325**: 1088–1098.
- Meng H, Song Y, Zhu J, Liu Q, Lu P, Ye N, Zhang Z, Pang Y, Qi J, Wu H (2016). LRG1 promotes angiogenesis through upregulating the TGF- $\beta 1$  pathway in ischemic rat brain. *Molecular Medicine Reports* **14**: 5535–5543.
- Nakajima M, Miyajima M, Ogino I, Wada S, Kano T, Kakinuma C, Ogihara T (2012). Brain localization of leucine-rich $\alpha 2$ -glycoprotein and its role. *Acta Neurochirurgica Supplement* **113**: 97–101. <https://doi.org/10.1007/978-3-7091-0923-6>
- Nguyen QL, Okuno N, Hamashima T, Dang ST, Fujikawa M et al. (2021). Vascular PDGFR- $\alpha$  protects against BBB dysfunction after stroke in mice. *Angiogenesis* **24**: 35–46. <https://doi.org/10.1007/s10456-020-09742-w>
- Otxoa-de-Amezaga A, Miró-Mur F, Pedragosa J, Gallizioli M, Justicia C et al. (2019). Microglial cell loss after ischemic stroke favors brain neutrophil accumulation. *Acta Neuropathologica* **137**: 321–341. <https://doi.org/10.1007/s00401-018-1954-4>
- Pek SL, Tavintharan S, Wang X, Lim SC, Woon K, Yeoh LY, Ng X, Liu J, Sum CF (2015). Elevation of a novel angiogenic factor, leucine-rich- $\alpha 2$ -glycoprotein (LRG1), is associated with arterial stiffness, endothelial dysfunction, and peripheral arterial disease in patients with type 2 diabetes. *The Journal of Clinical Endocrinology and Metabolism* **100**: 1586–1593. <https://doi.org/10.1210/jc.2014-3855>
- Sarfraz A, Javeed M, Shah MA, Hussain G, Shafiq N et al. (2020). Biochanin A: A novel bioactive multifunctional compound from nature. *The Science of the Total Environment* **722**: 137907. <https://doi.org/10.1016/j.scitotenv.2020.137907>
- Su EJ, Cao C, Fredriksson L, Nilsson I, Stefanitsch C et al. (2017). Microglial-mediated PDGF-CC activation increases cerebrovascular permeability during ischemic stroke. *Acta Neuropathologica* **134**: 585–604. <https://doi.org/10.1007/s00401-017-1749-z>
- Tsai CF, Chen GW, Chen YC, Shen CK, Lu DY, Yang LY, Chen JH, Yeh WL (2021). Regulatory effects of quercetin on M1/M2 macrophage polarization and oxidative/antioxidative balance. *Nutrients* **14**: 67. <https://doi.org/10.3390/nu14010067>
- Wang H, Hong LJ, Huang JY, Jiang Q, Tao RR et al. (2015). P2RX7 sensitizes Mac-1/ICAM-1-dependent leukocyte-endothelial adhesion and promotes neurovascular injury during septic encephalopathy. *Cell Research* **25**: 674–690. <https://doi.org/10.1038/cr.2015.61>

- Wu WY, WZ, Wang HL, Chen HQ, Yin YY (2015). Biochanin A attenuates LPS-induced pro-inflammatory responses and inhibits the activation of the MAPK pathway in BV2 microglial cells. *International Journal of Molecular Medicine* **35**: 391–398. <https://doi.org/10.3892/ijmm.2014.2020>
- Wu D, Deng S, Li L, Liu T, Zhang T, Li J, Yu Y, Xu Y (2021). TGF- $\beta$ 1-mediated exosomal lnc-MMP2-2 increases blood-brain barrier permeability via the miRNA-1207-5p/EPB41L5 axis to promote non-small cell lung cancer brain metastasis. *Cell Death & Disease* **12**: 721. <https://doi.org/10.1038/s41419-021-04004-z>
- Wu LY, Ye ZN, Zhuang Z, Gao Y, Tang C et al. (2018). Biochanin A reduces inflammatory injury and neuronal apoptosis following subarachnoid hemorrhage via suppression of the TLRs/TIRAP/MyD88/NF- $\kappa$ B pathway. *Behavioural Neurology* **2018**: 1960106. <https://doi.org/10.1155/2018/1960106>
- Xia Y, Hu G, Chen Y, Yuan J, Zhang J, Wang S, Li Q, Wang Y, Deng Z (2021). Embryonic stem cell derived small extracellular vesicles modulate regulatory T cells to protect against ischemic stroke. *ACS Nano* **15**: 7370–7385. <https://doi.org/10.1021/acsnano.1c00672>
- Xu L, Sun H, Zhang Y, Guo Z, Xiao X, Zhou X, Hu K, Sun W, Wang B, Liu W (2021). Proteomic analysis of human frontal and temporal cortex using iTRAQ-based 2D LC-MS/MS. *Chinese Neurosurgical Journal* **7**: 27. <https://doi.org/10.1186/s41016-021-00241-5>
- Xue HX, Kong H, Yu YG, Zhou JW, Chen HQ, Yin YY (2019). Biochanin A protects against angiotensin II-induced damage of dopaminergic neurons in rats associated with the increased endophilin A2 expression. *Behavioural Pharmacology* **30**: 700–711. <https://doi.org/10.1097/FBP.0000000000000515>
- Xue Z, Li A, Zhang X, Yu W, Wang J, Li Y, Chen K, Wang Z, Kou X (2020). Amelioration of PM2.5-induced lung toxicity in rats by nutritional supplementation with biochanin A. *Ecotoxicology and Environmental Safety* **202**: 110878. <https://doi.org/10.1016/j.ecoenv.2020.110878>
- Yamashita F, Sasaki M, Takahashi S, Matsuda H, Kudo K, Narumi S, Terayama Y, Asada T (2010). Detection of changes in cerebrospinal fluid space in idiopathic normal pressure hydrocephalus using voxel-based morphometry. *Neuroradiology* **52**: 381–386. <https://doi.org/10.1007/s00234-009-0610-z>
- Yang X, Liang J, Jia M, Yang T, Deng X et al. (2021).  $\beta$ -1, 3-galactosyltransferase 2 ameliorates focal ischemic cerebral injury by maintaining blood-brain barrier integrity. *Neurochemistry International* **144**: 104976. <https://doi.org/10.1016/j.neuint.2021.104976>
- Yin J, Zhang X, Zhang Y, Ma Y, Li L, Li D, Zhang L, Zhang Z (2019). Comprehensive study of the in vivo and in vitro metabolism of dietary isoflavone biochanin A based on UHPLC-Q-TOF-MS/MS. *Journal of Agricultural and Food Chemistry* **67**: 12481–12495. <https://doi.org/10.1021/acs.jafc.9b05776>
- Youn K, Park JH, Lee J, Jeong WS, Ho CT, Jun M (2016). The identification of biochanin A as a potent and selective  $\beta$ -site app-cleaving enzyme 1 (Bace1) inhibitor. *Nutrients* **8**: 637. <https://doi.org/10.3390/nu8100637>
- Zarmouh NO, Eyunni SK, Soliman KF (2017). The benzopyrone biochanin-A as a reversible, competitive, and selective monoamine oxidase B inhibitor. *BMC Complementary and Alternative Medicine* **17**: 34. <https://doi.org/10.1186/s12906-016-1525-y>
- Zhang M, Wang Y, Wang J, Li X, Ma A, Pan X (2021). Serum LRG1 as a novel biomarker for cardioembolic stroke. *Clinica Chimica Acta* **519**: 83–91. <https://doi.org/10.1016/j.cca.2021.04.002>
- Zheng R, Zhang ZH, Zhao YX, Chen C, Jia SZ, Cao XC, Shen LM, Ni JZ, Song GL (2019). Transcriptomic insights into the response of the olfactory bulb to selenium treatment in a mouse model of Alzheimer's disease. *International Journal of Molecular Sciences* **20**: 2998. <https://doi.org/10.3390/ijms20122998>
- Zou Y, Xu Y, Chen X, Wu Y, Fu L, Lv Y (2022). Research progress on leucine-rich alpha-2 glycoprotein 1: A review. *Frontiers in Pharmacology* **12**: 809225. <https://doi.org/10.3389/fphar.2021.809225>